J Radioanal Nucl Chem
DOI 10.1007/s10967-016-4766-9

Evaluating the applicability of portable-XRF for the characterization of Hokkaido Obsidian sources: a comparison with INAA, ICP-MS and EPMA

Sean C. Lynch[1] · Andrew J. Locock[2] · M. John M. Duke[3] · Andrzej W. Weber[1,4]

Received: 18 September 2015

Abstract As a result of the limited application of portable X-ray fluorescence (pXRF) in archaeological research in Japan it is necessary to compare this technique to proven, laboratory-based, analytical techniques. In this study instrumental neutron activation analysis, inductively-coupled plasma mass spectrometry, and electron probe microanalysis are used to validate pXRF and determine the overall suitability of this technique for archaeological obsidian provenance studies in Hokkaido, northern Japan. Furthermore, the results of this study are compared to previously published data to assess reproducibility and compatibility. This study demonstrates the reliability of pXRF for the rapid characterization of Hokkaido obsidian while contributing to the ongoing evaluation of the applicability of "off-the-shelf" pXRF to obsidian provenance research in archaeology.

Keywords pXRF · INAA · ICP-MS · EPMA · Obsidian · Hokkaido

✉ M. John M. Duke
mjduke@ualberta.ca

Sean C. Lynch
sclynch@ualberta.ca

[1] Department of Anthropology, University of Alberta, Edmonton, Canada

[2] Department of Earth and Atmospheric Sciences, University of Alberta, Edmonton, Canada

[3] SLOWPOKE Facility, University of Alberta, Edmonton, Canada

[4] Laboratoire Méditerranéen de Préhistoire Europe Afrique (LAMPEA), Aix-Marseille Université, Aix-en-Provence, France

Introduction

Since the early 2000's several studies have focused on the characterization of Hokkaido obsidian sources for archaeological applications using a variety of analytical techniques including instrumental neutron activation analysis (INAA), laboratory-based energy dispersive X-ray fluorescence (EDXRF) spectrometry, wavelength dispersive X-ray fluorescence (WDXRF) spectrometry, electron probe micro-analysis (EPMA) and laser-ablation inductively-coupled-plasma mass spectrometry (LA-ICP-MS) [1–12]. Fewer studies have explored the potential for the rapid characterization of Japanese obsidian using portable X-ray fluorescence (pXRF) [13–15].

There are 21 known sources, including sub-sources, of obsidian on Hokkaido Island, Japan (Fig. 1) [16]. Obsidian produces a very sharp natural edge after a fresh break, making it a highly desirable material for tool-making by prehistoric peoples. However, weathered (altered) obsidian is a less desirable material for the production of stone tools.

In Hokkaido, several obsidian deposits are known to contain high quality raw material suitable for the production of stone tools [7]. In particular, material from the Shirataki deposit has been used by prehistoric peoples in Hokkaido since approximately 30,000 years before present (YBP) [7, 16]. By about 19,000 YBP prehistoric people had transported obsidian from Hokkaido deposits over 1000 km from their sources [7]. The most prominent sources of obsidian on Hokkaido are Shirataki, Oketo, Akaigawa and Tokachi-Mistumata (Fig. 1). By determining the source of origin of obsidian artifacts, archaeologists may reconstruct prehistoric mobility patterns, as well as trade and exchange networks. An initial evaluation of pXRF for obsidian provenance research in Hokkaido has been provided by analyzing obsidian artifacts recovered

Published online: 11 March 2016

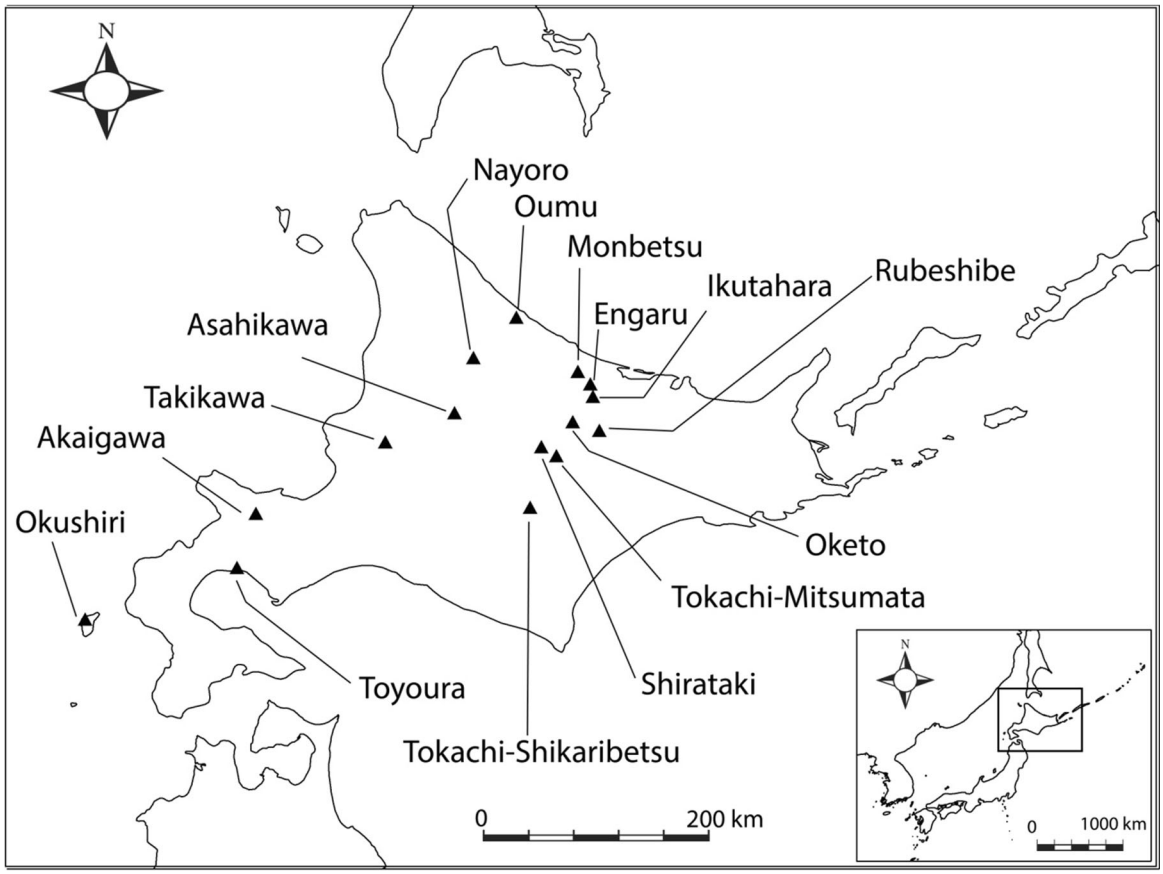

Fig. 1 Map of Hokkaido, Japan, with approximate locations of known obsidian sources

from the Kuril Islands [14]. However, this study [14] did not include original source data for Hokkaido deposits, and instead relied on 'legacy data' [17] from INAA [6] to determine the provenance of the analyzed artifacts. A recent study [13] provides a comparison between pXRF and INAA data and demonstrates the compatibility of these techniques for the characterization of Hokkaido obsidian source material. This latter study did not evaluate the pXRF with respect to other commonly used analytical techniques such as inductively-coupled-plasma mass spectrometry (ICP-MS) and EPMA. Furthermore, given that the bulk of elemental data for Hokkaido obsidian sources has been produced by the University of Missouri Research Reactor Archaeometry group (hereafter MURR), it seemed pertinent to evaluate the results of this group through the analysis of similar source material by an independent laboratory. In the present study, an obsidian sample from the Hokkaido Shirataki-Akaishiyama deposit is characterized by four independent techniques of elemental analysis, namely pXRF, INAA, ICP-MS and EPMA, to evaluate the compatibility of pXRF with these more traditional techniques, as well as to assess the limitations of pXRF.

Analytical methodology

EDXRF technology has been available in the form of relatively portable desktop units for decades [18]. However, miniaturization of this technology in the past decade into highly portable, handheld pXRF devices has encouraged the use of this technology for obsidian provenance studies in archaeology in the field. Recently, there has been a marked increase in use of pXRF devices in archaeology (e.g., [18–20]). Portable XRF uses the same operating principles as laboratory-based EDXRF instruments, providing researchers with a practical, highly portable, rapid, and non-destructive method of elemental analysis. Furthermore, this technology allows researchers to complete chemical analyses where archaeological collections are housed, foregoing the difficulty or impossibility of transporting collections of artifacts to research facilities abroad.

Despite the advantages of this technology, pXRF is not without limitations. The elemental sensitivity for pXRF devices varies, and can be affected by choice of X-ray tube target, operating accelerating voltage and current, the use of filters, as well as the option of analyzing samples in air,

vacuum, or helium atmospheres to enhance the detection of specific elements. Additionally, the calibration packages provided by manufacturers, or developed by users, together with sample shape and composition can impact the accuracy of results produced by these devices [20–23]. Furthermore, pXRF is known to be less sensitive, and hence has poorer detection limits, in comparison with established analytical methods of analysis such as INAA, ICP-MS, and higher power, bench-top XRF units [19], including wavelength dispersive XRF (WDXRF) equipment. This shortfall is particularly evident when utilizing pXRF to quantify elements with a lower atomic number than Ti. Nonetheless, pXRF has been shown to have sufficient sensitivity, accuracy and precision for differentiating obsidian sources, and for assigning artifact materials to their original geological formations when compared with established geochemical methods of analysis [24–26]. Trace elements, including Rb, Sr, and Zr, are of principal concern in obsidian provenance studies, given that the concentrations of these elements are often characteristic of individual deposits [27]. Despite the growing body of research in support of the accuracy and precision of pXRF analyses, debate over the reproducibility of pXRF results continues within the archaeological community [18–20, 22, 24–26]. Therefore, further examination of the compatibility of pXRF with established methods of analysis is considered worthwhile to confirm the reliability of pXRF results.

Experimental

Methods and materials

The obsidian specimen used in this study comes from the Shirataki-Akaishiyama deposit and was labelled JPN-1; it was acquired from Hokkaido University, Sapporo. Three colour-varieties of obsidian are found at the Shirataki-Akaishiyama deposit: red and black, reddish-brown, and jet-black [1]. However, these materials vary only slightly in their bulk chemical compositions despite their dissimilar appearances. Specimen JPN-1 is of the red and black variety of obsidian found at the summit of the Shirataki-Akasishiyama deposit. The Shirataki-Akaishiyama deposit was chosen for this study because of the significant volume of data previously obtained by benchmark geochemical techniques for this source. Specimen JPN-1 was initially analyzed multiple times by pXRF then subsequently analyzed by INAA, ICP-MS, and EPMA. In order to assess the accuracy of the INAA and ICP-MS determinations a sample of USGS RGM-1 (a rhyolite, similar in composition to JPN-1), was included in the batch of samples analyzed by both techniques.

Portable XRF

Sample JPN-1 was analyzed twenty-eight times over an eight week period using a Bruker AXS Tracer III-SD XRF analyzer equipped with a rhodium (Rh) X-ray tube and silicon drift detector (SDD) with a measured resolution of 148 eV FWHM for 5.9 keV X-rays. Operating conditions were as follows: accelerating voltage 40 kV and 30 μA beam current, with filtration of the primary X-rays by a polymetallic filter (0.3047 mm Al, 0.0254 mm Ti, 0.1523 mm Cu). Data acquisition was for 300 s live-time. In this study ten elements were quantified by pXRF; Mn, Fe, Zn, Ga, Rb, Sr, Y, Zr, and Nb were measured using their $K\alpha$ X-ray emissions, while Th was determined using its $L\alpha$ emission. Intensities were calculated as ratios to the Rh Compton peak and converted to μg/g using the Bruker AXS proprietary obsidian calibration [24]. This calibration is based on the analyses of 40 obsidian samples previously characterized by INAA and LA-ICP-MS and provides a broad range of elemental concentrations for obsidian source material from around the world.

Sample preparation

For analysis by INAA and ICP-MS, random flakes from specimen JPN-1 were ground under acetone using an agate mortar and pestle to less than 200 mesh-size generating about 12 g of ground obsidian, also labelled JPN-1. For EPMA additional pieces of specimen JPN-1 were used, for which a flat surface was prepared by grinding and polishing. Electron probe micro-analysis was used to quantify the major and minor elements of the glass and inclusions of JPN-1, as opposed to its trace element composition, and to assess sample heterogeneity at the micron-level using back-scattered electron (BSE) mapping.

INAA

INAA was performed at the University of Alberta SLOWPOKE-II Nuclear Reactor Facility. Aliquots of samples and standards, each weighing between 470 and 530 mg, were weighed into individual nitric acid washed 0.75 mL polyethylene irradiation vials and hermetically sealed. The samples were irradiated sequentially in an inner site of the SLOWPOKE Nuclear Reactor for 240 s at a nominal thermal neutron flux of 1×10^{11} n cm^{-2} s^{-1}. Following a timed decay period (typically 15–20 min) each sample was counted for 240 s at a sample-to-detector distance of 20 cm utilizing a 40 % relative efficiency ORTEC FX-Profile hyperpure Ge detector with carbon window, attached to an ORTEC DSPEC Pro digital spectrometer. Measurements with the spectrometer were performed in zero dead time mode for loss free counting.

Following a ~5 day decay period the samples and standards were simultaneously re-irradiated (two batches of three samples per 7 mL irradiation vial) for 2 h at a nominal thermal neutron flux of 5×10^{11} n cm^{-2} s^{-1}. Each sample was subsequently counted twice using a 40 % ORTEC FX-Profile detector; the initial count was for 3000 s live-time, at a sample-to-detector distance of 3 cm, following a 6 day decay period, and a second measurement for 50,000 s live-time, following a decay period of at least 2 weeks. The second, extended count, was performed with the sample positioned transversely to the detector face, on a protective end cap cover.

Element quantification was performed by the semi-absolute comparator method of NAA [28] using standard reference materials of known composition from NIST (1633a, flyash) and CANMET (SY-4, diorite gneiss). Utilizing the analysis protocols described above Al, Ba, Ce, Co, Cs, Eu, Fe, Hf, La, Lu, Mn, Na, Nd, Rb, Sb, Sc, Sm, Sr, Ta, Tb, Th, Yb, Zn and Zr were determined. In addition to these elements, Si and U were measured on a single 300 mg aliquot of JPN-1 employing fast- and epithermal-NAA, respectively. The aliquot was weighed into a 300 uL polyethylene micro-centrifuge tube, hermetically sealed, placed in the central cavity of a ^{10}B-enriched shield, and irradiated in an inner site of the SLOWPOKE reactor. Quantification of Si and U were performed utilizing the 1273.4 and 74.7 keV gamma emissions of ^{29}Al ($T½ = 6.56$ min) and ^{239}U ($T½ = 23.47$ min), respectively. Silicon and U were determined using the semi-absolute comparator method of NAA utilizing Brazilian Corinto quartz and NIST 1633a, respectively, for Si and U quantification.

ICP-MS

Ground samples, each weighing approximately 200 mg, were dissolved in a mixture of 8 mL HF and 2 mL HNO_3 in a closed vessel at 130 °C for 48 h and subsequently dried in an open vessel at 140 °C. The residue was digested in a mixture of 5 mL HCl and 5 mL HNO_3 in a closed vessel at 130 °C for 24 h and dried again in an open vessel at 140 °C. The residue was taken up in 10 mL of 8 N HNO_3 in preparation for analysis by solution mode ICP-MS with sample dilution occurring just prior to analysis.

Diluted sample solutions were run on a Perkin Elmer Elan 6000 quadrupole ICP-MS. The running conditions included a sample flow rate of 1 mL per minute, 35 sweeps per reading, with three replicates and one reading per replicate. Dwell times of 10 ms were used in the determination of Zn and Sr, whereas 20 ms dwell times were used for all other elements. The ICP RF power was 1300 W, and the instrument was run in dual detector mode with the auto lens on. Four-point calibration curves were used for each element.

EPMA

Electron microprobe data were acquired on a JEOL 8900 instrument operated at 15 kV and 10 nA, with a beam diameter of 10 μm for analysis of obsidian and 1 μm for other phases. Count times for wavelength-dispersive spectrometry were 20 s on peaks and 10 s on backgrounds for the $K\alpha$ lines of the following elements (standards in parentheses): Na (albite), Mg and Ca (diopside), Al and Si (Lipari obsidian), P (apatite), K (sanidine), Ti (rutile), Mn (rhodonite), and Fe (hematite). Data were reduced using CITZAF [29]. Back-scattered-electron (BSE) mapping of two polished and carbon-coated (25 nm thickness of C) pieces of obsidian was completed in eleven square sections for a total area of 68.9 mm^2 at a nominal pixel width of 2.44 μm.

Results

The results from the pXRF, INAA, and ICP-MS analyses of specimen JPN-1 are provided in Tables 1, 2 and 3. The analyses of specimen JPN-1 by pXRF show a low relative standard deviation (RSD) for the elements examined, demonstrating good instrumental precision and stability over an 8 week period (Table 1). A single aliquot of the United States Geological Survey (USGS) reference material RGM-1 (rhyolite) was analyzed by both INAA and ICP-MS to evaluate accuracy and examine inter-method variability. All elemental concentration values in μg/g were rounded based on their analytical precision.

The ICP-MS Rb result for RGM-1 showed a positive bias of 14 % compared to the accepted Rb concentration

Table 1 pXRF results for JPN-1. Concentrations in μg/g, except for Fe (wt%)

Element	Mean ± 1σ ($n = 28$)	RSD %
Mn	598 ± 26	4.4
Fe (%)	0.93 ± 0.02	2.1
Zn	65 ± 3	4.5
Ga	35 ± 1.4	4.0
Th	22 ± 1	4.9
Rb	146 ± 3	2.3
Sr	31 ± 1	3.1
Y	33 ± 0.7	2.2
Zr	78 ± 1.1	1.4
Nb	13.9 ± 0.5	3.9

Table 2 INAA results for JPN-1 and RGM-1, and values for USGS RGM-1 [30]

Element	JPN-1 ($n = 3$)	RGM-1 ($n = 1$)	USGS RGM-1
Na (%)	2.90 ± 0.06	2.86 ± 0.07	3.02 ± 0.11
Al (%)	6.74 ± 0.09	7.24 ± 0.08	7.26 ± 0.10
Si (%)	35.15 ± 0.75*	ND	34.30 ± 0.25
Fe (%)	0.835 ± 0.008	1.27 ± 0.01	1.30 ± 0.04
Mn	390 ± 7	292 ± 4	282 ± 30
Zn	34 ± 1	35 ± 1	32 ± 6
Rb	151 ± 1	147 ± 1	149 ± 8
Sr	28 ± 2	99 ± 6	108 ± 10
Zr	84 ± 2	214 ± 8	219 ± 20
Th	11.5 ± 0.1	14.2 ± 0.1	15.1 ± 1.3
Sc	2.76 ± 0.03	4.43 ± 0.01	4.4 ± 0.3
Co	0.61 ± 0.08	2.57 ± 0.04	2.0 ± 0.2
La	22.6 ± 0.7	24.2 ± 0.1	24.0 ± 1.1
Ce	41.5 ± 0.6	51.4 ± 0.2	47 ± 4
Nd	17.1 ± 0.4	18.5 ± 0.2	19 ± 1
Sm	4.04 ± 0.07	4.47 ± 0.02	4.3 ± 0.3
Eu	0.30 ± 0.02	0.63 ± 0.02	0.66 ± 0.08
Tb	0.67 ± 0.01	0.60 ± 0.02	0.66 ± 0.06
Yb	2.83 ± 0.05	2.33 ± 0.03	2.6 ± 0.3
Lu	0.449 ± 0.002	0.396 ± 0.003	0.41 ± 0.03
Cs	9.87 ± 0.18	9.96 ± 0.05	9.6 ± 0.6
Ta	0.59 ± 0.01	0.92 ± 0.02	0.95 ± 0.10
Ba	897 ± 6	843 ± 6	807 ± 46
Hf	2.87 ± 0.03	6.32 ± 0.03	6.2 ± 0.3
Sb	0.39 ± 0.05	1.67 ± 0.04	1.26 ± 0.07
U	3.39 ± 0.06*	ND	5.8 ± 0.5

ND not determined

* Determination on a single aliquot

Table 3 ICP-MS results for JPN-1 and RGM-1, and values for USGS RGM-1 [30]

Element	JPN-1 ($n = 3$)	RGM-1 ($n = 1$)	USGS RGM-1
Mn	360 ± 9	421	282 ± 30
Fe (%)	0.80 ± 0.03	1.37	1.30 ± 0.04
Zn	26 ± 0.6	29	32 ± 6
Ga	16 ± 0.3	18	15 ± 2
Rb	152 ± 2	149	149 ± 8
Sr	28 ± 2	106	108 ± 10
Y	25 ± 1	21	25 ± 4
Zr	64 ± 1	219	219 ± 20
Nb	7 ± 0.3	11	8.9 ± 0.6
Th	15 ± 1	27	15.1 ± 1.3

for this rock standard [30]. A review of possible isobaric interferences [31] with Rb offered no explanation for the bias which is considered most likely to be due to systematic error. Consequently, an empirical correction factor based on this measured bias, was applied to the measured ICP-MS Rb results for the triplicate JPN-1 determinations. With the correction factor applied the ICP-MS Rb results for JPN-1 are in excellent agreement with those determined by pXRF and INAA.

While some fifty-five elements were measured by ICP-MS given that the focus of this paper is the evaluation of pXRF for obsidian analysis only those elements common to both pXRF and ICP-MS are considered here. Elements, additional to those quantified utilizing the Bruker pXRF obsidian calibration, determined by INAA are reported here for comparison with Hokkaido obsidian INAA results previously published [7].

Back-scattered-electron (BSE) imaging using a fully focussed beam (<1 μm diameter) on the electron microprobe revealed numerous inclusions in the obsidian (Fig. 2), ranging in size from about 50 μm diameter down to <0.5 μm (the approximate limit of instrumental resolution). As the inclusions are generally at or below the pixel size of the BSE mapping (2.44 μm), quantitative image analysis of these maps is not warranted.

Analyses of iron oxides were acquired for inclusions greater than 10 μm in size in the BSE-mapped areas. Table 4 lists the averages of the analyses of hematite (Fe_2O_3) and magnetite (Fe_3O_4) inclusions that have less than 1.0 wt% SiO_2 (minimal contamination from the host obsidian). In addition to the abundant iron oxide inclusions, a few examples of laihunite [32] enveloped by iron oxides were noted (Table 4), as was a single aggregate consisting of apatite, zircon, and monazite-(Ce).

For the obsidian matrix, 270 quantitative analyses were obtained by EPMA, along with 28 analyses of a Lipari obsidian standard. Although efforts were made to avoid sub-micron inclusions of hematite-rich material, the matrix obsidian analyses showed a range from 0.15 to 0.70 wt% FeO (note that for the obsidian, iron is reported as FeO). Table 5 lists the average and standard deviation of these analyses, along with analyzed data and recommended values for the Lipari obsidian [33]. The results for the Shirataki obsidian are similar to those previously determined by EPMA [11, 12].

Bulk determinations of the major element composition of the Shirataki-Akaishiyama obsidian from both the literature and the present work are listed in Table 6. The composition of the obsidian matrix glass determined by electron microprobe (Table 5) differs significantly in SiO_2 and FeO from the mean bulk composition listed in Table 6. Most of the inclusions observed in the obsidian consist of iron oxides (Fig. 2).

The mean iron content of the obsidian matrix is 0.33 wt% FeO (Table 5), and those of ideal hematite and magnetite (expressed here as ferrous oxide) are 89.98, and 93.08 wt% FeO, respectively. The mean bulk

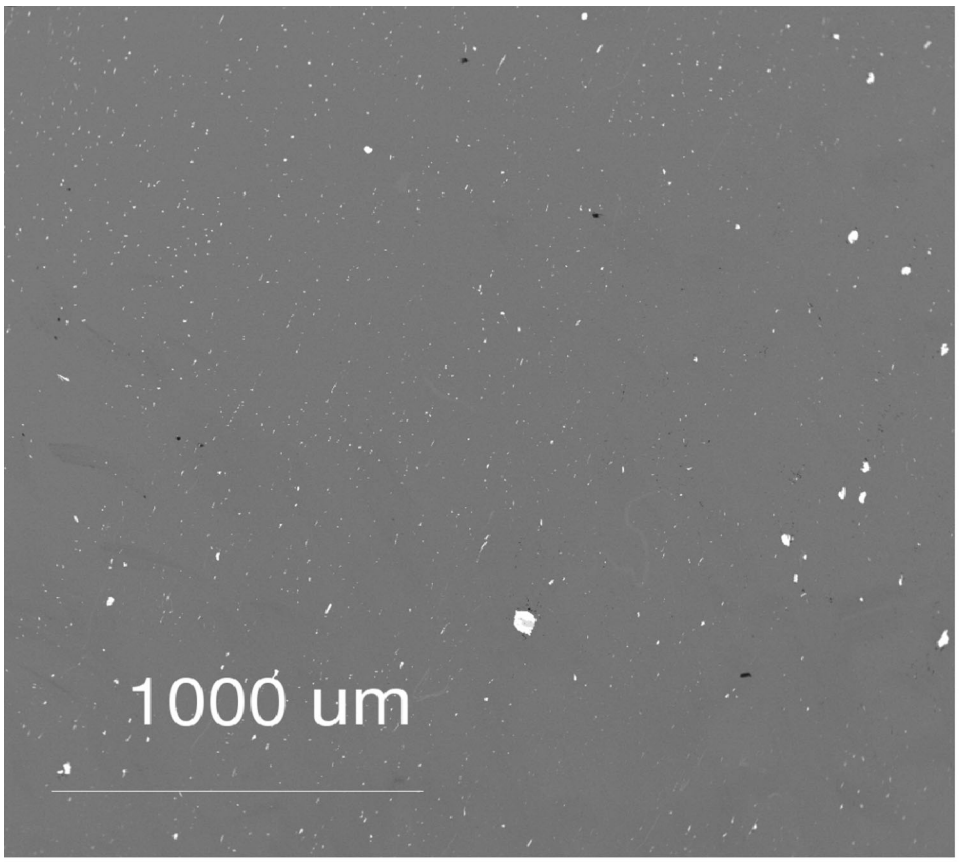

Fig. 2 BSE image of JPN-1: *white spots* are iron oxides and iron silicates

Table 4 EPMA data of hematite, magnetite, and laihunite

wt%	Hematite ($n = 20$)	Magnetite ($n = 8$)	Laihunite ($n = 6$)
SiO_2	0.52 ± 0.21	0.50 ± 0.21	34.85
TiO_2	0.03 ± 0.04	0.02 ± 0.02	
Al_2O_3	1.18 ± 0.27	1.96 ± 0.43	
MnO	0.39 ± 0.30	0.67 ± 0.13	1.92
Fe_2O_3	97.29 ± 0.72	65.79 ± 0.97	55.92
FeO	0.20 ± 0.24	30.80 ± 0.14	4.99
MgO	0.09 ± 0.08	0.39 ± 0.08	0.46
CaO	0.03 ± 0.02	0.03 ± 0.02	
Total	99.73 ± 0.50	100.15 ± 0.41	98.14

concentration of FeO is 1.10 wt% FeO (Table 6). If the matrix obsidian and the iron oxide inclusions are the only significant contributors to the bulk iron concentration, then their relative proportions by weight are about 99.15–99.20 %, and 0.80–0.85 %, respectively. Assuming ideal densities of 2.2 g/cm^3 for the obsidian matrix [34], and 5.26 g/cm^3 for hematite and 5.18 g/cm^3 for magnetite, the relative proportions of the matrix obsidian and the iron oxide inclusions by volume are 99.6 and 0.4 %, respectively.

Table 5 EPMA data of obsidian matrix and Lipari standard

wt %	Mean ($n = 270$)	Lipari ($n = 28$)	Lipari [33]
SiO_2	77.11 ± 0.33	74.06 ± 0.31	74.1 ± 0.7
TiO_2	0.04 ± 0.02	0.08 ± 0.02	0.07 ± 0.01
Al_2O_3	13.26 ± 0.09	13.40 ± 0.10	13.1 ± 0.2
MnO	0.05 ± 0.02	0.07 ± 0.02	0.07 ± 0.02
FeO	0.33 ± 0.12	1.47 ± 0.07	1.55 ± 0.03
MgO	0.03 ± 0.01	0.04 ± 0.02	0.04 ± 0.01
CaO	0.54 ± 0.04	0.72 ± 0.02	0.73 ± 0.03
Na_2O	3.68 ± 0.16	3.80 ± 0.11	4.07 ± 0.11
K_2O	4.42 ± 0.08	5.01 ± 0.11	5.11 ± 0.13
P_2O_5	0.02 ± 0.02	0.01 ± 0.02	0.01 ± 0.01
Total	99.48 ± 0.42	98.66 ± 0.44	98.85 ± 0.77

Discussion

The INAA data determined at the University of Alberta for JPN-1 are compared in Fig. 3 with previous INAA data reported for the Shirataki-Akaishiyama deposit [7]. As demonstrated by the correlation coefficient and slope the two data sets are in excellent agreement (with the exception Co), demonstrating inter-laboratory consistency for a

Table 6 Compilation of major element abundances of Shirataki-Akaishiyama Obsidian

References	Method	SiO_2	TiO_2	Al_2O_3	MnO	FeO
[1]	EDXRF					1.43
[6]	INAA			12.48		1.02
[3]	INAA			12.75		1.03
[2]	INAA			12.75		1.02
[2]	EDXRF					0.90
[9]	WDXRF	77.19	0.04	12.97	0.05	1.32
[7]	INAA			12.85		1.01
UAB	INAA	75.2		12.74	0.05	1.07
UAB	ICP-MS					1.03
UAB	PXRF					1.20
Average		76.20	0.04	12.76	0.05	1.10

References	MgO	CaO	Na_2O	K_2O	P_2O_5	Total
[1]						
[6]			3.98	4.66		
[3]			3.88	4.49		
[2]			3.88	4.49		
[2]						
[9]	0.01	0.53	3.91	4.57	0.02	100.61
[7]			3.87	4.60		
UAB			3.90			
UAB						
UAB						
Average	0.01	0.53	3.90	4.56	0.02	99.17

UAB University of Alberta

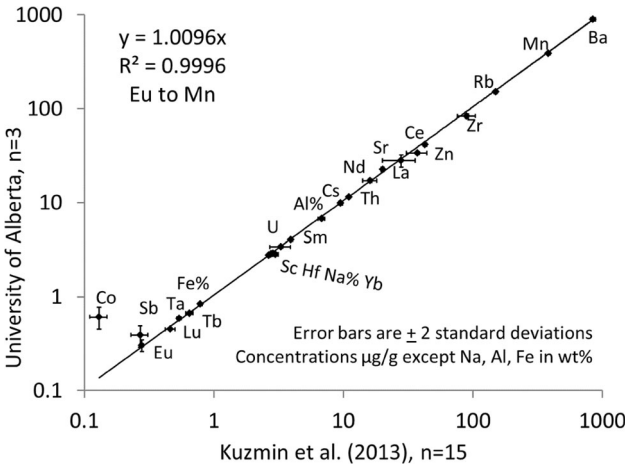

Fig. 3 Comparison of University of Alberta INAA data with Kuzmin et al. [7]

wide range of elements for the Shirataki-Akaishiyama obsidian sub-deposit. Therefore, the MURR and University of Alberta INAA data for the Shirataki-Akaishiyama deposit are deemed reliable and reproducible. One of the basic tenets of obsidian sourcing is that obsidian, or individual flows of obsidian, are homogeneous at the macroscopic level (i.e., elemental analysis sampling and artifact scale). The BSE image (Fig. 2) and EPMA of the JPN-1 inclusions (Table 4) and obsidian matrix (Table 5) demonstrate that the JPN-1 obsidian is heterogeneous at the microscopic scale. However, based on the agreement between the JPN-1 INAA results presented here with those from MURR for the same obsidian source [7], together with the low pXRF elemental %RSDs (±1.4–4.9 %) obtained in this study (Table 1), JPN-1 is considered homogeneous at the macroscopic (hand-specimen) scale.

The elemental analyses of this study demonstrate the consistency of pXRF data with INAA and ICP-MS results for the trace elements Rb, Sr, and Zr that are important for obsidian source determination [35]. In contrast, the concentrations of elements, such as Mn, Zn and Ga, show relatively poor agreement with those established by the other techniques (Tables 1, 2 and 3). The inaccuracy of the pXRF data for these latter elements may be partly attributed to the uneven surface of the JPN-1 sample examined. The processes of X-ray generation and detection are strongly influenced by sample surface morphology [22, 36]. The Bruker pXRF obsidian calibration, based on the analysis of samples with a flat sample geometry, appears to result in an over-estimation of the lower energy X-ray lines (Mn to Ga, in this case), when applied to irregularly shaped samples. Flat or polished sample surfaces are the ideal for pXRF analysis. However, prehistoric obsidian artifacts are typically irregular in shape and lack flat surfaces. Thus, the JPN-1 sample selected for this study is morphologically irregular, reflecting the common real-world experience of archaeologists who may use pXRF for the analysis of archaeological samples. Despite this complication, the petrologically important trace elements that have proven valuable in obsidian source determination (Rb, Sr, Zr) [35] were accurately and precisely quantified by pXRF in this study.

Conclusions

In an assessment of the Bruker Tracer pXRF obsidian calibration Speakman [24] noted that "…it is the responsibility of the PXRF user to evaluate and modify any factory calibrations as appropriate (or generate their own) to ensure that data are valid and reliable." This study demonstrates the consistency of pXRF data with INAA and ICP-MS results for the trace elements Rb, Sr and Zr, which known to be important elements for obsidian source determination [35]. In contrast, the pXRF results for the concentrations of elements such as Mn, Zn and Ga are only in fair agreement with those established by the other techniques. The EPMA data are found to be in good

agreement with the INAA and ICP-MS data, as well as previously published results for the Shirataki-Akaishiyama deposit. The analysis of specimen JPN-1 by INAA at the University of Alberta SLOWPOKE Reactor Facility was found to be in excellent agreement with other INAA data [7] for Shirataki-Akaishiyama obsidian. Given the agreement between the pXRF and INAA and ICP-MS data for the trace elements Rb, Sr and Zr reported here, and published in previous studies for the Shirataki-Akaishiyama deposit, pXRF (using a Bruker Tracer III-SD XRF analyzer) is deemed a reliable and accurate methodology for the characterization of Hokkaido obsidian. Therefore, pXRF will likely become a valuable method of analysis for future obsidian provenance research in Hokkaido.

The BSE maps determined by EPMA demonstrate that obsidian, ostensibly homogeneous at the macroscopic level, can be heterogeneous at the microscopic level. Bulk elemental analysis of obsidian, using techniques such as INAA and ICP-MS and employing representative ground samples, are typically insensitive to, and unaffected by, such microscopic heterogeneities. As the size of the X-ray beam striking a sample in this study is an ellipse, some 8 mm by 6 mm in size, microscopic heterogeneities are not considered a concern when analyzing obsidian by pXRF. However, it must be kept in mind that the depth of penetration, and depth from which characteristic X-rays can escape a sample, varies depending upon the composition of the sample and energy of the primary and secondary X-rays involved. Given the relatively energetic nature of the characteristic X-rays detected in this study (5.9 keV [Mn] to 16.6 keV [Nb]) the microscopic heterogeneities identified in the JPN-1 obsidian are considered to be insignificant in the pXRF elemental determinations. This contention is supported by the low variation (%RSD) seen for the 28 analyses of JPN-1 performed over an 8 week period.

The advantages of pXRF for obsidian source determination, compared to laboratory-based analytical techniques, are its portability, rapidity of analysis, and non-destructive nature; features which are important considerations for an archaeologist who conducts research in remote areas, or who is otherwise unable to transport collections to research facilities. The other analytical methods used here all require some degree of sample preparation, whether sizing to fit in a reactor irradiation vial (INAA), polishing of a thin section or mount (EPMA), or the removal, crushing and dissolution of a representative sample (ICP-MS). Thus, whole artifacts, or portions thereof, must be marred or partially destroyed in order to be analyzed. Despite the limitations on the accuracy for some elements, pXRF is shown to be a powerful and adequate analytical method for rapid, non-destructive, obsidian source determination in Hokkaido, Japan particularly when employing the trace elements Rb, Sr, and Zr.

Acknowledgments The pXRF work described here was made possible through funding from the Canada Foundation for Innovation. Funding contributions were also provided by the Baikal-Hokkaido Archaeology Project, the University of Alberta, the Department of Anthropology, and the Canadian Circumpolar Institute. Hirofumi Kato, Masayuki Mukai and Tetsuhiro Tomoda are acknowledged for the logistical support they provided in Hokkaido.

References

1. Hall M, Kimura H (2002) Quantitative EDXRF studies of obsidian sources in northern Hokkaido. J Archaeol Sci 29:259–266
2. Glascock MD, Kuzmin YV, Grebennikov AV, Popov VK, Medvedev VE, Shewkomud IY, Zaitsev NN (2011) Obsidian provenance for prehistoric complexes in the Amur River basin (Russian Far East). J Archaeol Sci 38:1832–1841
3. Kuzmin YV, Glascock MD (2007) Two islands in the ocean: prehistoric obsidian exchange between Sakhalin and Hokkaido, northeast Asia. J Island Coast Archaeol 2:99–120
4. Kuzmin YV (2006) In: Dumond DE, Bland RL (eds) Archaeology of northeast Asia: on the pathway to the Bering Strait. University of Oregon, Eugene
5. Kuzmin YV (2010) In: Kuzmin YV, Glascock MD (eds) Crossing the straits: prehistoric obsidian source exploitation in the north Pacific Rim. Archaeopress, Oxford
6. Kuzmin YV, Glascock MD, Sato H (2002) Sources of archaeological obsidian on Sakhalin Island (Russian Far East). J Archaeol Sci 29:741–749
7. Kuzmin YV, Glascock MD, Izuho M (2013) The geochemistry of the major sources of archaeological obsidian on Hokkaido Island (Japan): Shirataki and Oketo. Archaeometry 55:355–369
8. Phillips SC (2010) In: Kuzmin YV, Glascock MD (eds) Crossing the straits: prehistoric obsidian source exploitation in the north Pacific Rim. Archaeopress, Oxford
9. Suda Y (2012) Chemical analysis of obsidian by wavelength-dispersive X-ray fluorescence spectrometry: application to non-destructive analysis of archeological obsidian artifacts. Nat Resour Environ Hum 2:1–14
10. Tomura K, Koshimizu T, Nishimoto T (2003) Instrumental neutron activation analysis for the source estimation of obsidian samples from the site of Hamanaka 2, Rebun Island, Hokkaido. Bull Natl Mus Jpn Hist 107:189–196
11. Wada K, Mukai M, Takeda O (2003) Chemical compositions of obsidian glasses determined by EPMA: the origin of obsidians from the remains at the mouth of Tokoro River, eastern Hokkaido. Reports of Taisetsuzan Institute of Science, Hokkaido University of Education. 37:59–70
12. Wada K, Shibuya R, Yamaya F, Mukai M (2006) Source of the obsidian artifacts at the Rishirifuji Town Hall site, Rishiri Island, northern Hokkaido: major element compositions of the obsidian glasses determined by the EPMA. Reports of Taisetsuzan Institute of Science, Hokkaido University of Education. 40:27–39
13. Ferguson JR, Glascock MD, Izuho M, Mukai M, Wada K, Sato H (2014) In: Ono A, Kuzmin YV, Suda Y (eds) Methodological issues for characterization and provenance studies of obsidian in northeast Asia. Archaeopress, Oxford
14. Phillips SC, Speakman RJ (2009) Initial source evaluation of archaeological obsidian from the Kuril Islands of the Russian Far East using portable-XRF. J Archaeol Sci 36:1256–1263
15. Lynch SC (2013) Portable-XRF analysis of archaeological obsidian from Rebun Island, Japan. MA Thesis, Department of Anthropology, University of Alberta, Edmonton

16. Izuho M, Hirose W (2010) In: Kuzmin YV, Glascock MD (eds) Crossing the straits: prehistoric obsidian source exploitation in the north Pacific Rim. Archaeopress, Oxford
17. Forster N, Grave P (2012) Non-destructive PXRF analysis of museum-curated obsidian from the Near East. J Archaeol Sci 39:729–736
18. Shackley MS (2010) Is there reliability and validity in portable X-ray fluorescence spectrometry (PXRF)? SAA Archaeol Rec. 10:17–20
19. Freund KP (2013) An assessment of the current applications and future directions of obsidian sourcing studies in archaeological research. Archaeometry 55:779–793
20. Speakman RJ, Shackley MS (2013) Silo-science and portable-XRF in archaeology: a response to Frahm. J Archaeol Sci 40:1435–1443
21. Davis M, Jackson T, Shackley MS, Teague T, Hampel J (2011) In: Shackley MS (ed) X-ray fluorescence spectrometry (XRF) in geoarchaeology. Springer, New York
22. Ferguson JR (2012) In: Shugar AN, Jennifer L (eds) Mass studies in archaeological sciences: handheld XRF for art and archaeology. Leuven University Press, Leuven
23. Goodale N, Bailey DG, Jones GT, Prescott C, Scholz E, Stagliano M, Lewis C (2012) PXRF: a study of inter-instrument performance. J Archaeol Sci 39:875–883
24. Speakman RJ (2012) Evaluation of Bruker's Tracer Family Factory Obsidian calibration for handheld portable XRF studies of obsidian. Report prepared for Bruker AXS, Kennewick. https://www.bruker.com/fileadmin/user_upload/8-PDF-Docs/X-rayDiffraction_ElementalAnalysis/HH-XRF/LabReports/Bruker_Obsidian_Report.pdf. Accessed 15 Sept 2015
25. Frahm E (2013) Validity of "off-the-shelf" handheld portable-XRF for sourcing Near Eastern obsidian chip debris. J Archaeol Sci 40:1080–1092
26. Frahm E (2013) Is obsidian sourcing about geochemistry or archaeology? A reply to Speakman and Shackley. J Archaeol Sci 40:1444–1448
27. Tykot RH (2004) In: Martini M, Milazzo M, Piacentini M (eds) Proceedings of the international school of physics. IOS Press, Amsterdam
28. Bergerioux C, Kennedy G, Zikovsky L (1979) Use of the semi-absolute method in neutron activation analysis. J Radioanal Chem 50:229–234
29. Armstrong JT (1995) CITZAF: a package of correction programs for the quantitative electron microbeam X-ray-analysis of thick polished materials, thin-films, and particles. Microbeam Anal 4:177–200
30. Gladney ES, Roelandts I (1988) Compilation of elemental concentration data for USGS BHVO-1, MAG-1, QLO-1, RGM-1, SCo-1, SDC-1, SGR-1, and STM-1. Geostandard Newslett 12:253–362
31. May TW, Wiemeyer RH (1998) A table of polyatomic interferences in ICP-MS. At Spectrosc 19:150–155
32. Xu H, Shen Z, Konishi H, Fu P, Szlufarska I (2014) Crystal structures of laihunite and intermediate phases between laihunite-1*M* and fayalite: Z-contrast imaging and ab initio study. Am Mineral 99:881–889
33. Kuehn SC, Froese DG, Shane PAR, Intercomparison Participants INTAV (2011) The INTAV intercomparison of electron-beam microanalysis of glass by tephrochronology laboratories: results and recommendations. Quat Intl 246:19–47
34. George WO (1924) The relation of the physical properties of natural glasses to their chemical composition. J Geol 32:353–372
35. Hancock RGV, Carter T (2010) How reliable are our published archaeometric analyses? Effects of analytical techniques through time on the elemental analysis of obsidians. J Archaeol Sci 37:243–250
36. Marckowicz AA (2008) In: Potts PJ, West M (eds) Portable X-ray fluorescence spectrometry. Royal Society of Chemistry, Cambridge